Instantaneous normal mode analysis of correlated cluster motions in hydrogen bonded liquids

G. Garberoglio and R. Vallauri[a)]
Istituto Nazionale di Fisica della Materia and Dipartimento di Fisica, Università degli Studi di Trento, I-38050 Povo (TN), Italy

G. Sutmann
Research Center Jülich, Central Institute for Applied Mathematics and John von Neumann Institute for Computing, D-52425 Jülich, Germany

(Received 11 October 2001; accepted 22 May 2002)

We analyze the correlated motions of hydrogen bonded clusters in liquid hydrogen fluoride, methanol, and water using the Instantaneous Normal Mode approach. In the case of hydrogen fluoride and methanol, which form a topologically linear hydrogen bond network, the relevant cluster is a triplet formed by a molecule and its two neighbors. In the case of water, whose hydrogen bond structure has a local tetrahedral symmetry, the basic unit considered is the pentamer formed by a molecule and its four neighbors. For each of these clusters we identify, using symmetry arguments, the *a priori* modes describing the relative motions of the cluster molecules and introduce suitable projections in order to evaluate how much these modes contribute to the actual motions at different frequencies. In the case of hydrogen fluoride we confirm the assignment of a 50 rad/ps peak observed in the single and collective correlation function spectra to the stretching of the hydrogen bonded network. In the case of methanol the analysis of the correlated motions of the triplets shows that in the intermediate frequency range (around 25 rad/ps) a picture similar to what is observed in hydrogen fluoride applies, whereas the high frequency properties of the liquid (beyond 50 rad/ps) are mostly due to the asymmetric stretching motion. In the case of water we demonstrate that the *a priori* modes, based on the full tetrahedral symmetry of the water pentamer, do indeed mix strongly under the effect of the interaction with the neighbors. The results are related to the spectroscopic measurement. © *2002 American Institute of Physics.* [DOI: 10.1063/1.1493775]

I. INTRODUCTION

The interest in the physics of hydrogen bonded liquids is mainly driven by the overwhelming importance of water and aqueous solutions in various branches of science and technology, ranging from chemistry and biology to industrial applications.

These systems are different from simple (monatomic) liquids since their structure, as well as the dynamics, is mostly determined by the anisotropic contributions to the interaction potential due to the presence of strong directional bonds. As a matter of fact the local coordination number of any given molecule is much lower than in simple liquids (e.g., Ar, where it is of the order of 12), depending on the number of hydrogen bonds that one molecule is able to form. As is well known, at ambient conditions each water molecule in the liquid state is coordinated, on the average, with other four hydrogen bonded molecules disposed in a tetrahedral fashion, and this particular arrangement is thought to be responsible for some of the ''unusual'' properties of this liquid, both from a static[1] and dynamic[2] point of view.

It is then interesting to investigate whether some peculiar behavior is also present in other hydrogen bonded liquids having different hydrogen bond topologies. Among the simplest of these systems are hydrogen fluoride and methanol; for both of them the average coordination number is two and the hydrogen bond network is formed by long topological chains.[3–6]

From the point of view of the dynamical properties, both of these systems present unusual features in the high frequency part of the spectra of the velocity autocorrelation function[7–11] or the density–density correlation function,[12,13] at least when compared with the dynamical behavior of simple monatomic liquids (e.g., Lennard-Jones systems).

In this respect the Instantaneous Normal Mode (INM) approach[14] is a very interesting tool for understanding the physical processes underlying the peculiar dynamical properties. As we shall explain later, this method, based on the harmonic approximation to the potential energy surface, provides an exact description of the short-time dynamics of a liquid. Moreover, from the diagonalization of the quadratic form which approximates the true potential energy, it is possible to analyze, at the various frequencies (the square root of the eigenvalues) the actual motions of the particles (given by the corresponding eigenvectors).

This interesting feature of the INM approach has been exploited in some recent studies[15–18] by performing suitable projections of the motions described by the eigenvectors according to some *a priori* behavior. One can then have, from the corresponding eigenvalues, an indication of the fre-

a)Author to whom correspondence should be addressed. Electronic mail: vallauri@science.unitn.it

quency ranges where the motion to be tested is more important.

To the best of our knowledge few papers dealing with this subject have appeared concerning the study of ionic melts[18] and vitreous systems.[17,19]

In the case of the systems under consideration we have already used this method to determine the effects of the hydrogen bond on the single molecule dynamics, by splitting the INM density of states (DOS) into translational and rotational contributions, which are further separated according to the single particle motion along relevant directions in the molecular reference frame.[15,16] In the same papers we have also presented an analysis based on the correlated motions of pairs of hydrogen bonded molecules.

In the present work we extend this picture to describe the various contributions to the INM DOS arising from the internal motions of clusters of hydrogen bonded molecules. In the case of linear chain forming liquids (hydrogen fluoride and methanol) the relevant clusters are formed by triplets of bonded molecules.

In the case of water we discuss also the more relevant case of structure of five coordinated molecules (pentamers). The average four neighbors of any molecule can be further distinguished into two categories. Two molecules ''donate'' their hydrogen bonds, since their H atoms point toward the O atom of the central molecule, and the two other molecules ''accept'' a hydrogen bond each, since the H atoms of the central molecule point toward their O atoms. In this sense the hydrogen bonded network can be separated in *accepted* or *donated* triplets and the analysis that we have performed for linear chain forming liquids can be applied.

This paper is organized as follows: in Sec. II we briefly review the Instantaneous Normal Mode theory. We define also the internal *a priori* modes of triplets and pentamers and introduce the projection operators which allow us to investigate to which extent the various *a priori* modes contribute to the dynamics at different frequencies. In Sec. III we describe the simulated system we have used for the analysis, together with the various numerical methods employed and the definition of the hydrogen bond used to identify triplets and pentamers. In Sec. IV we analyze, in terms of the INM, the motion induced by the presence of the hydrogen bonds at the level of triplets of coordinated molecules. This analysis is extended to the case of water pentamers in Sec. V, where we also compare the results of the full INM analysis with the projection on restricted modes obtained considering isolated pentamers only. This allows us to establish to which extent the internal modes of a pentamer are affected by the interaction with the surrounding environment. In Sec. VI we summarize the results obtained.

II. INSTANTANEOUS NORMAL MODES AND *A PRIORI* MODES

Let us denote by $q_{i\mu}$ the μth coordinate of the ith particle in a given configuration, by d the number of degrees of freedom of each molecule and N the number of molecules in the system under consideration. The translational coordinates of the ith molecules correspond to the index value $\mu=1,2,3$ and the rotational ones to $\mu=4,5,6$, the latter value only for nonlinear molecules. In what follows we have used as rotational coordinates the angles of rotation around the instantaneous direction of the principal inertia axes of any molecule, since this choice has been demonstrated to avoid the presence of spurious modes.[20]

The INM approach is based on the following expansion of the potential energy V around a given configuration $\mathbf{q}_0$:

$$V(\mathbf{q}_0+\delta\mathbf{q})=V(\mathbf{q}_0)-\mathbf{F}(\mathbf{q}_0)\cdot\delta\mathbf{q}+\tfrac{1}{2}\delta\mathbf{q}\cdot\mathsf{H}\cdot\delta\mathbf{q}+\cdots, \quad (1)$$

where $\mathbf{F}$ denotes the generalized forces and the matrix H is the Hessian.

The equations of motion for the displacements $\delta\mathbf{q}$ is then

$$\mathsf{T}\delta\ddot{\mathbf{q}}=\mathbf{F}-\mathsf{H}\cdot\delta\mathbf{q}, \quad (2)$$

where T is the mass matrix of the system. With the choice of rotational coordinates described above this matrix is diagonal, its entries being the total mass and the principal inertia moments of the molecule.

We can now pass on to the *mass weighted* coordinates, defined as

$$\delta m_{i\mu}=\sqrt{T_{i\mu,i\mu}}\,\delta q_{i\mu} \quad (3)$$

and the equation of motion in these new coordinates is

$$\delta\ddot{\mathbf{m}}=\mathsf{T}^{1/2}\mathbf{F}-\mathsf{D}\cdot\delta\mathbf{m}, \quad (4)$$

where

$$D_{i\mu,j\nu}=\frac{H_{i\mu,j\nu}}{\sqrt{T_{i\mu,i\mu}T_{j\nu,j\nu}}} \quad (5)$$

is now a symmetric matrix whose elements have the dimension of a squared frequency. If we denote by U the orthogonal matrix such that $\Omega^2=\mathsf{U}^{\dagger}\mathsf{D}\mathsf{U}$ is diagonal we can define new coordinates, the Instantaneous Normal Modes,

$$\mathbf{e}=\mathsf{U}\delta\mathbf{m} \quad (6)$$

whose equation of motion is

$$\ddot{\mathbf{e}}=\mathbf{f}-\Omega^2\mathbf{e}, \quad (7)$$

where the INM forces are defined as

$$\mathbf{f}=\mathsf{U}\mathsf{T}^{1/2}\mathbf{F}. \quad (8)$$

The initial conditions of Eq. (7) are given by

$$\mathbf{e}(0)=0=\mathsf{U}\mathsf{T}^{1/2}\delta\mathbf{q}(0), \quad (9)$$

$$\dot{\mathbf{e}}(0)=\mathbf{v}=\mathsf{U}\mathsf{T}^{1/2}\delta\dot{\mathbf{q}}(0), \quad (10)$$

where the components of the eigenmode velocities $\mathbf{v}$ obey, due to the equipartition theorem, to the relation,

$$\langle v_\alpha v_\beta\rangle=k_BT\delta_{\alpha\beta}. \quad (11)$$

The solution for the αth component is, denoting with $\omega_\alpha^2=\Omega_{\alpha,\alpha}^2$ the squared eigenfrequency,

$$e_\alpha(t)=\frac{f_\alpha}{\omega_\alpha^2}[1-\cos(\omega_\alpha t)]+\frac{v_\alpha}{\omega_\alpha}\sin\omega_\alpha t. \quad (12)$$

We would like to notice that the αth row of the U matrix

contains the normalized mass-weighted displacements of the particles according to the αth eigenmode. Since we need, for each molecule i a vector describing its center-of-mass displacement according to the αth mode we introduce the quantity,

$$\mathbf{u}_i^\alpha = (\mathsf{U}_{\alpha,i1}, \mathsf{U}_{\alpha,i2}, \mathsf{U}_{\alpha,i3}). \tag{13}$$

The translational and rotational contribution to the DOS,

$$\rho(\omega) = \left\langle \frac{1}{dN} \sum_\alpha \delta(\omega - \omega_\alpha) \right\rangle \tag{14}$$

are given by

$$\rho_T(\omega) = \left\langle \frac{1}{dN} \sum_\alpha \sum_{i=1}^{N} \sum_{\mu=1}^{3} [U_{\alpha,i\mu}]^2 \delta(\omega - \omega_\alpha) \right\rangle, \tag{15}$$

$$\rho_R(\omega) = \left\langle \frac{1}{dN} \sum_\alpha \sum_{i=1}^{N} \sum_{\mu=4}^{d} [U_{\alpha,i\mu}]^2 \delta(\omega - \omega_\alpha) \right\rangle, \tag{16}$$

respectively. From the normalization of the eigenmodes, it is easy to see that $\rho(\omega) = \rho_T(\omega) + \rho_R(\omega)$. In fact inspection of Eqs. (15) and (16) shows that the translational and rotational projections are just the DOS (14) weighted with the contribution of the translational or rotational degrees of freedom to each mode, respectively.

These ''projections'' can further be extended to investigate the anisotropy of the local environment as a function of the mode frequency.[15] If we denote by $\mathbf{w}_i$ a vector defined for each molecule i (e.g., the direction of one of the principal inertia axis of the molecule), we can build the weighted DOS,

$$\rho_w(\omega) = \left\langle \sum_\alpha \sum_{i=1}^{N} \sum_{\mu=1}^{3} [U_{\alpha,i\mu} w_{i\mu}]^2 \frac{\delta(\omega - \omega_\alpha)}{dN} \right\rangle. \tag{17}$$

If the local environment were isotropic we would expect $\rho_w(\omega) = \rho_T(\omega)/3$. Since this is not likely to be the case when dealing with H-bonded systems, due to the strongly directional bonds, the projections of the translational DOS along various $\mathbf{w}_i$ vectors can give a clear picture of how these bonds influence the dynamics at various frequencies.[15]

Since expansion (1) is not performed from a configuration of mechanical equilibrium the Hessian matrix (and its mass-weighted form) is not positive definite, not all the squared eigenfrequencies are positive. In the case of negative eigenfrequencies the sine and cosine function in Eq. (12) must be substituted by hyperbolic sine and cosine, respectively. For these frequencies the displacement described by the INM approach is an exponential departure from the given configuration, and this fixes the range of temporal validity.

As a matter of fact the expansion (1) cannot hold for an arbitrarily long time since the study of the dynamical behavior of liquids has to take into account the rearrangement of the whole structure induced by collisional processes. The frequency (or temporal) range of validity of the INM approach is then to be found in the ''collision frequency'' between the molecules. At the density typical of liquid systems the particles are always interacting, however the inverse of the Einstein frequency can be taken as a measure of the ''time between collisions.'' [21] As a matter of fact the highest modulus of the imaginary modes is always found to be of the same order of the Einstein frequency for both simple[22] and molecular liquids.[15,16]

In this work we will be mainly concerned with dynamical properties occurring at frequencies of the order of or higher than the Einstein frequency of the systems under consideration, which is $\Omega_0 \simeq 24$ rad/ps for methanol, $\Omega_0 \simeq 33$ rad/ps for HF, and $\Omega_0 \simeq 37$ rad/ps for water at the state points considered, so that our conclusions are hardly affected by the approximation (1) to the true interaction potential.

A. The *a priori* triplet motions

We define a triplet to be composed of a central molecule (C) and its two hydrogen bonded neighbors to be called, conventionally, left (L) and right (R).

We show in Fig. 1 the coordinate systems used in the description of a given triplet, whose molecules are supposed to be at the vertices of an equilateral triangle. We will see afterwards what has to be changed if we were to consider the fact that, in a disordered system such as a liquid, we are not likely to find molecules in such a symmetric arrangement.

For the left and right molecules we define a unit vector, ψ_L and ψ_R, respectively, in the direction of the central molecule. The vector product $\zeta = \psi_L \times \psi_R$, denotes the direction orthogonal to the plane defined by the three molecules. For each of the molecules in the triplet we define a vector ξ_i ($i = L,R,C$ in the case of left, right, or central molecule, respectively) pointing in the direction of the triplet's center-of-mass. We further define $\eta_i = \zeta_i \times \xi_i$ and, for the left and central molecules, two unit vectors π_i orthogonal to the ''bond'' direction ψ_i, and lying in the triplet's plane, $\pi_i = \zeta_i \times \psi_i$.

The possible motions of the translational coordinates of a triplet are described by 9 degrees of freedom and consequently the normal modes of such a cluster can be described by a set of nine nine-dimensional vectors $\mathbf{P}^{(k)}$ which obey the standard completeness and orthogonality relations. We use the convention that the first three entries of these vectors describe the motion of the central molecule of the cluster, the next three the motion of the left molecule, and the remaining three the motion of the right one.

Three of these normal mode vectors describe the rigid translation in the three spatial directions,

$$\mathbf{P}^{(1)} = \frac{1}{\sqrt{3}}[1,0,0;1,0,0;1,0,0],$$

$$\mathbf{P}^{(2)} = \frac{1}{\sqrt{3}}[0,1,0;0,1,0;0,1,0], \tag{18}$$

$$\mathbf{P}^{(3)} = \frac{1}{\sqrt{3}}[0,0,1;0,0,1;0,0,1],$$

while three other vectors describe the *rigid rotation* of the

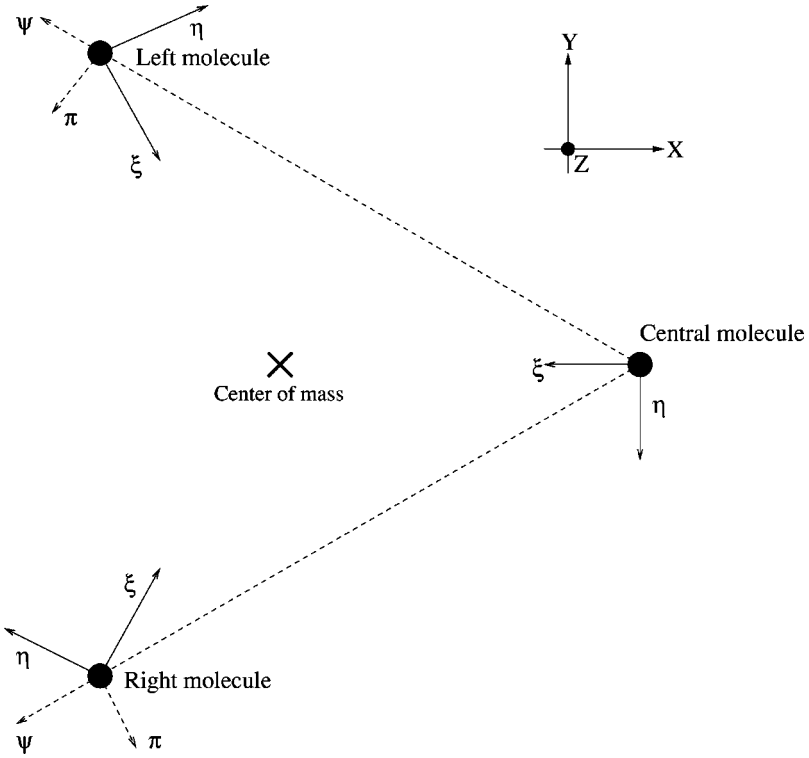

FIG. 1. The coordinates used in describing the triplet motions.

cluster, with respect to the ζ_C, ξ_C, and η_C axis, respectively,

$$\mathbf{P}^{(4)}=\frac{1}{\sqrt{3}}[\eta_C;\eta_L;\eta_R],$$

$$\mathbf{P}^{(5)}=\frac{1}{\sqrt{2}}[0,0,0;-\zeta_L;\zeta_R], \tag{19}$$

$$\mathbf{P}^{(6)}=\sqrt{\frac{2}{3}}\left[-\zeta_C;\frac{\zeta_L}{2};\frac{\zeta_R}{2}\right],$$

for the symmetric cluster we are considering the last three vectors describe the internal motions, which can be divided in symmetric stretching, asymmetric stretching and bending, given, respectively, by

$$\mathbf{P}^{(7)}=\mathbf{P}^{S}=\frac{1}{\sqrt{3}}[\xi_C;\xi_L;\xi_R],$$

$$\mathbf{P}^{(8)}=\mathbf{P}^{A}=\frac{1}{\sqrt{3}}[\eta_C;-\psi_L;\psi_R], \tag{20}$$

$$\mathbf{P}^{(9)}=\mathbf{P}^{B}=\frac{1}{\sqrt{3}}[-\xi_C;\pi_L;-\pi_R],$$

and shown in Fig. 2.

We can now describe how to take into account the fact that, in liquid configurations, the triplets are not likely to be found in such symmetric configuration. First of all we notice that the definition of the ψ, ξ, ζ, η, and π vectors does indeed depend only on the relative direction between the cluster's

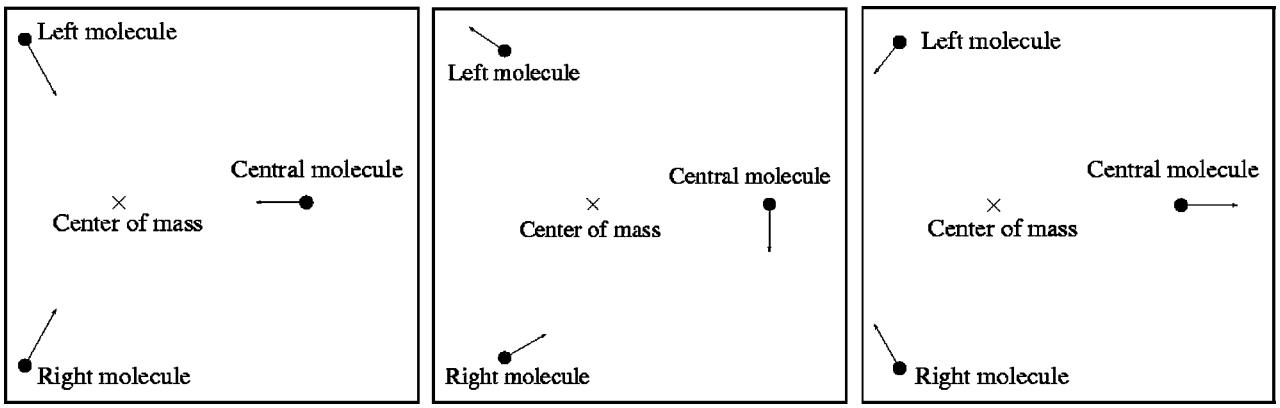

FIG. 2. From left to right: the molecular motion corresponding to the symmetric stretching mode, the asymmetric stretching mode, and the bending mode.

molecules and not on the supposed symmetry. We also notice that the assignment of the internal motions to bending or stretching depends only on the fact that we are considering the relative motion of each molecule in the triplets with respect to the others.

From these considerations we deduce that the bending or stretching character of the modes is preserved even if the triplet does not possess the full symmetry.

The only problem that arises in the general case is the fact that the *a priori* modes that we define analogously to the symmetric situation are not necessarely orthogonal to the three translational modes. Any projection on the internal modes for general triplet will then include also the motion of the center-of-mass, which we would like to avoid since we are interested only in the relative motion of the particles.

We have then decided, whenever we will project out *a priori* modes on the actual Instantaneous Modes of the system, to subtract the center-of-mass motion of the triplet given by the Instantaneous Mode under consideration.

B. The *a priori* pentamer motions

The *a priori* modes of pentamers are described by a 15-dimensional vector. The first three entries represent the displacement of the central molecule (which we label as 0), and the other twelve denote the displacement of the remaining molecules, which are labeled by the numbers 1–4.

There are essentially four kinds of motion, and we take their definition from Taraskin and Elliott,[17] with only one change: in our *a priori* modes we allow the central molecule to move, and its displacement $\mathbf{x}_i$ is just the negative of the sum of the displacements of all the others. The index i here labels the mode under consideration.

This definition is necessary since the pentamers in a liquid configuration are not expected to have a perfect tetrahedral symmetry. By allowing the central molecule to move we assure that the *a priori* motions are orthogonal to the rigid translations, thus representing only the internal motion.

The *a priori* pentamer modes are then:

Symmetric stretch: the outer molecules move toward the central one. This is also known as ''breathing mode'' and has degeneracy one,

$$\mathbf{P}^S=\frac{1}{\sqrt{5}}[\mathbf{x}_S;\xi_1;\xi_2;\xi_3;\xi_4], \tag{21}$$

where ξ_i is a unit vector pointing from molecule i toward the center-of-mass of the cluster.

Asymmetric stretch: two outer molecules move away and two toward the central one. Its degeneracy is 3,

$$\begin{aligned}\mathbf{P}^{A1}&=\frac{1}{\sqrt{5}}[\mathbf{x}_{A1};\xi_1;\xi_2;-\xi_3;-\xi_4],\\ \mathbf{P}^{A2}&=\frac{1}{\sqrt{5}}[\mathbf{x}_{A2};\xi_1;-\xi_2;\xi_3;-\xi_4],\\ \mathbf{P}^{A3}&=\frac{1}{\sqrt{5}}[\mathbf{x}_{A3};\xi_1;-\xi_2;-\xi_3;\xi_4].\end{aligned} \tag{22}$$

Bending: Two outer molecules bend ''away'' and two ''toward'' each other. Its degeneracy is 3. In the following we will denote by $\mathbf{b}_{ij}$ a unit vector orthogonal to the distance from the ith molecule to the central one and directed toward the jth molecule,

$$\begin{aligned}\mathbf{P}^{B1}&=\frac{1}{\sqrt{5}}[\mathbf{x}_{B1};\mathbf{b}_{12};\mathbf{b}_{21};-\mathbf{b}_{34};-\mathbf{b}_{43}],\\ \mathbf{P}^{B2}&=\frac{1}{\sqrt{5}}[\mathbf{x}_{B2};\mathbf{b}_{14};-\mathbf{b}_{23};-\mathbf{b}_{32};\mathbf{b}_{41}],\\ \mathbf{P}^{B3}&=\frac{1}{\sqrt{5}}[\mathbf{x}_{B2};\mathbf{b}_{13};-\mathbf{b}_{24};\mathbf{b}_{31};-\mathbf{b}_{42}].\end{aligned} \tag{23}$$

The last two modes describe *Torsion* and are given by

$$\begin{aligned}\mathbf{P}^{T1}&=C_1[\mathbf{x}_{T1};2\mathbf{b}_{12}-\mathbf{b}_{13}-\mathbf{b}_{14};2\mathbf{b}_{21}-\mathbf{b}_{23}\\ &\quad-\mathbf{b}_{24};2\mathbf{b}_{34}-\mathbf{b}_{31}-\mathbf{b}_{32};2\mathbf{b}_{43}-\mathbf{b}_{41}-\mathbf{b}_{41}],\\ \mathbf{P}^{T2}&=C_2[\mathbf{x}_{T2};\mathbf{b}_{13}-\mathbf{b}_{14};-\mathbf{b}_{23}-\mathbf{b}_{24};\mathbf{b}_{31}-\mathbf{b}_{32};\\ &\quad-\mathbf{b}_{41}-\mathbf{b}_{42}],\end{aligned} \tag{24}$$

where C_1 and C_2 are normalization contants.

In any of the modes the vector $\mathbf{x}_i$ corresponding to the motion of the central molecule, has been built for each pentamer so that the corresponding mode is orthogonal to the ones describing rigid translation in the three spatial directions.

C. Projection on the *a priori* motions

Given the *a priori* modes discussed in the previous section, we can project onto them the actual motion of the clusters (triplets or pentamers) in the various eigenmodes.

For each cluster C of n molecules we build a $3n$-dimensional vector with the displacement of the constituent molecules relative to the αth eigenmode. If we denote by C_i the ith molecule ($i=1\cdots n$) of the Cth cluster we define

$$\mathbf{E}_\alpha^{(C)}=[\mathbf{u}_{C_1}^\alpha;\mathbf{u}_{C_2}^\alpha;\ldots;\mathbf{u}_{C_n}^\alpha], \tag{25}$$

where the vectors $\mathbf{u}_i^\alpha$ describe the center of mass displacement of the ith particle in the αth mode and are given by Eq. (13) since, according to our definitions, the αth row of the U matrix contains the normalized mass-weighted displacements of the particles according to the αth eigenmode.

We also need a vector whose components are the INM center-of-mass velocities of the same particles moving accordingly to the αth mode,

$$\mathbf{V}^{(C)}(t)=[\mathbf{v}_{C_1}(t);\mathbf{v}_{C_2}(t);\ldots;\mathbf{v}_{C_n}(t)], \tag{26}$$

where the velocities in the INM framework are given by Eq. (10),

TABLE I. Parameters used in the simulation.

Molecule	Number of particles	Density (g/cm^3)	Temperature (K)
Hydrogen fluoride	256	1.178	203
Methanol	216	0.8511	200

$$v_{i\mu}(t)=\sum_{\alpha} T^{-1/2}_{i\mu,i\mu}U_{\alpha,i\mu}\dot{e}_{\alpha}(t). \tag{27}$$

The mean value of the temporal correlation of the projection of the velocities onto the $\mathbf{P}^{(k)}$ mode is then

$$\frac{k_BT}{M}\phi_k(t)\equiv\nu\left\langle\frac{1}{n_C}\sum_{C=1}^{n_C}[\mathbf{V}^{(C)}(0)\cdot\mathbf{P}^{(k)}][\mathbf{V}^{(C)}(t)\cdot\mathbf{P}^{(k)}]\right\rangle, \tag{28}$$

where n_C is the number of clusters in a given configuration and ν is a normalizing factor, chosen by the requirement that $\Sigma_k\phi_k(0)=1$: $\nu=(nd)^{-1}$ (d is the number of degrees of freedom per molecule).

Using the solution of the INM dynamics and the statistical independence between the various components of the velocity, and definining the projection of the INM motion on the kth mode of pentamer P as

$$p_{\alpha}^{(k,C)}=\mathbf{E}_{\alpha}^{(C)}\cdot\mathbf{P}^{(k)}, \tag{29}$$

we can write the spectrum of the previous Eq. (28) as

$$\phi_k(\omega)=\left\langle\sum_{\alpha}\frac{N}{nn_C}\sum_{C}[p_{\alpha}^{(k,C)}]^2\frac{\delta(\omega-\omega_{\alpha})}{6N}\right\rangle. \tag{30}$$

This last equation can be directly interpreted as an INM spectrum weighted with the average projection of the particles' motion on the kth *a priori* mode of the cluster.

III. DETAILS OF THE SIMULATIONS

A. Hydrogen fluoride and methanol

We present the results obtained by molecular dynamics simulations on model systems. In the case of HF we use the pair potential developed by Jedlovszky and Vallauri[23] and in the case of methanol the Optimized Potential for Liquid Simulation (OPLS) developed by Jorgensen.[3]

We report in Table I the parameters used in the simulations. We have integrated the equation of motions in the NVE ensemble, using a time step of 1 fs. The long range Coulomb interaction between the molecules is taken into account by a reaction field method with conducting boundary conditions.

To evaluate the INM, we saved, in the case of methanol, 40 configurations separated by 3 ps each (these are the same configurations used in our previous work[16]) and, in the case of HF, we saved 70 configurations separated by 3 ps.

In order to identify hydrogen bonded pairs, we have used the same criterion adopted elsewhere,[15,16] namely, two molecules are considered hydrogen bonded if both of the following conditions are met:

(1) The center-of-mass distance must be <2.64 Å for HF and 3.8 Å for methanol (the first minimum of the center of mass pair distribution function);
(2) The interaction energy of the pair must be <-15.0 kJ/mol for HF and -12.6 kJ/mol for methanol.

B. Water

We have simulated a system of 256 SPC/E water molecules at a density of 1 g/cm^3. The integration has been performed with the weak coupling to a heat bath,[24] with a preset temperature of 300 K. We saved 60 configurations separated by 25 ps each for the INM analysis.

We consider two molecules to be hydrogen bonded if all of the following conditions are met in the liquid configurations:

(1) the O···H–O angle is $<35°$;
(2) interaction energy is <-9.64 kJ/mol;
(3) O···O distance is <3 Å;
(4) the previous conditions are satisfied during 1 ps trajectory.

From the knowledge of the bonding state between each pair of molecules we can then extract the various cluster types. In the case of triplets of hydrogen bonded molecules we can further distinguish between accepted and donated triplets.[25] In the former case the central molecule accepts two bonds (i.e., the hydrogens of the two other molecules point toward the oxygen atom of the central one), whereas in the latter the central molecule donates two bonds (i.e., its hydrogens point towards the oxygen atoms of the other two molecules).

In order to clarify the geometry of the various clusters, we show in Fig. 3 the probability for the angle formed by the two vectors pointing from the central molecule to the right and left one, and the probability distribution for the difference of the bond lengths, measured as the distance between the center-of-mass of two bonded molecules, both for accepted and donated triplets.

In the case of donated triplets we notice that the angle is very close to the tetrahedral one, probably due to the fact that for the SPC/E model this is the angle between the two hydrogens in the water molecule. In the case of accepted triplets the probability function is rather asymmetric and it is peaked at a value which is 30° less than the ideal tetrahedral angle.

The distribution of the difference of the bond lengths is peaked around zero, as expected, and has a pronounced non-Gaussian shape, with a corresponding standard deviation of $\simeq 0.25$ Å in both cases.

C. Calculation of the INM

The calculation of the INM has been performed by numerical evaluation of the Hessian matrix, using the formula,

$$\mathsf{H}_{i\mu,j\nu}=\frac{f_{i\mu}(\mathbf{q}_{j\nu}+h)-f_{i\mu}(\mathbf{q}_{j\nu}-h)}{2h}, \tag{31}$$

where $f_{i\mu}(\mathbf{q}_{j\nu}+h)$ is the generalized force acting on the coordinate $i\mu$ when the coordinate $j\nu$ is displaced by an

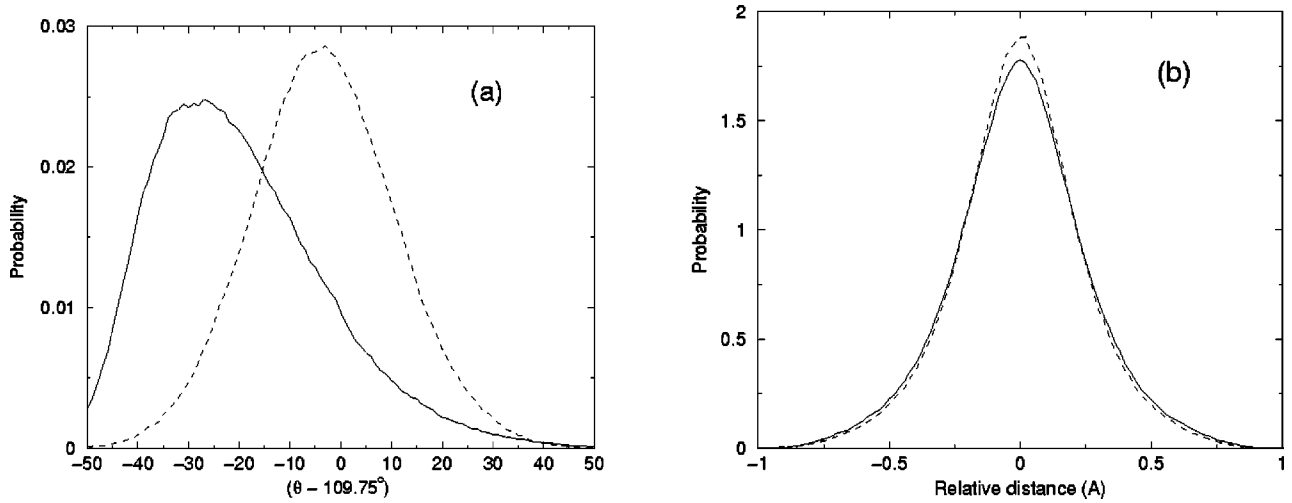

FIG. 3. (a) Probability distribution for the triplet angle for accepted (solid line) and donated (dashed line) triplets. (b) Probability distribution for the difference of the hydrogen bond lengths between the two outer molecules for accepted (solid line) and donated (dashed line) triplets.

amount h. We used $h=10^{-5}$ Å and we have checked the accuracy of this choice by the fact that no unusually high eigenvalues appear and by the presence of three purely translational modes at zero frequency ($\pm 10^{-6}$). The resulting Hessian matrix (in mass-weighted coordinates) has been diagonalized using standard methods.[26]

The INM DOS spectra that we have obtained, together with the translational and rotational contributions are in very good agreement with other studies appeared in the literature.[27,28]

IV. TRIPLET MOTIONS

A. Hydrogen fluoride and methanol

In previous works we have performed an INM analysis of the local molecular motions involved in the high frequency modes of HF (Ref. 15) and methanol[16] with particular emphasis on the single particle properties and nearest neighbor pair correlations. We have been able to conclude that the high frequency translational modes in HF (around 50 rad/ps) are indeed due to stretching motions localized on the H-bond chain structure, and a similar behavior has also been found in liquid methanol. In the latter case, however, the hydrogen bond stretching appeared to involve two frequencies: a lowest one at 25 rad/ps, corresponds to a pronounced shoulder in both the velocity autocorrelation and longitudinal current correlation spectra, whereas a higher frequency contribution (above 60 rad/ps) appears in the form of a long tail (see Ref. 16, and references therein). We can now shed more light on the exact kind of motions involved by using the projection on the triplet modes.

In the case of HF we show in Fig. 4 the projection on the asymmetric, symmetric stretching and bending modes given by Eq. (20).

We notice that the stretching motions, which are the ones mostly related to the dynamics ruled by the presence of strong directional H-bonds, contribute mostly in the high frequency range of the spectrum. Indeed the asymmetric stretching reaches a maximum around 50 rad/ps, while the symmetric stretching reaches a maximum at a slightly lower frequency (around 40 rad/ps). This is consistent with our previous findings[15] that assigned the excitations in this frequency range to the H-bond stretching.

On the other hand the projection on the bending mode gives the most important contribution at lower frequencies, reaching a maximum at 10 rad/ps. This is consistent with the fact that the restoring force for this kind of motion is directed almost perpendicularly to the H-bond direction and it is weaker than the one involved in the stretching modes.

We notice, moreover, that the projection on the bending motion gives the most important contribution to the imaginary modes, being almost twice the sum of the other two contributions. This means that the molecules are indeed strongly directionally bonded and that local diffusion mostly takes place with motions orthogonal to the H-bond direction.

The results for methanol, reported in Fig. 5, indicate a similar picture. The projection on the bending motion is pre-

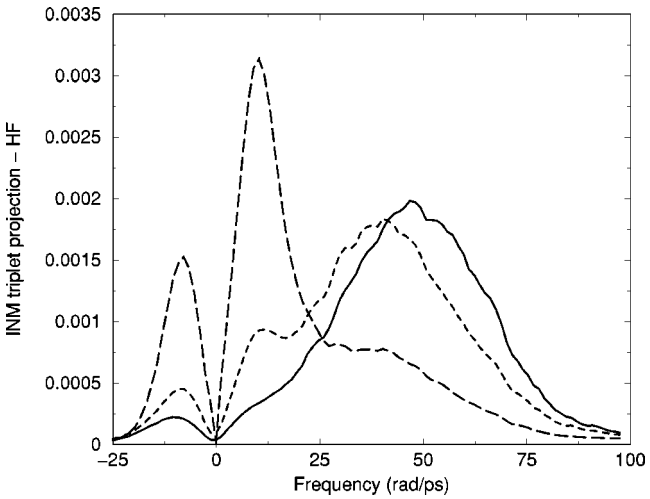

FIG. 4. Projection of the INM on the triplet modes for liquid HF. Solid line: asymmetric stretching; short-dashed line: symmetric stretching; dashed line: bending. The imaginary frequencies are reported on the negative axis, as usual.

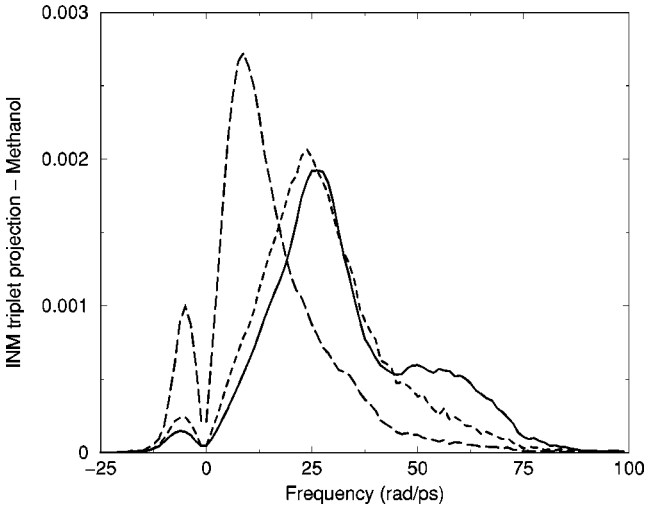

FIG. 5. Projection of the INM on the triplet modes for liquid methanol. Solid line: asymmetric stretching; short-dashed line: symmetric stretching; dashed line: bending.

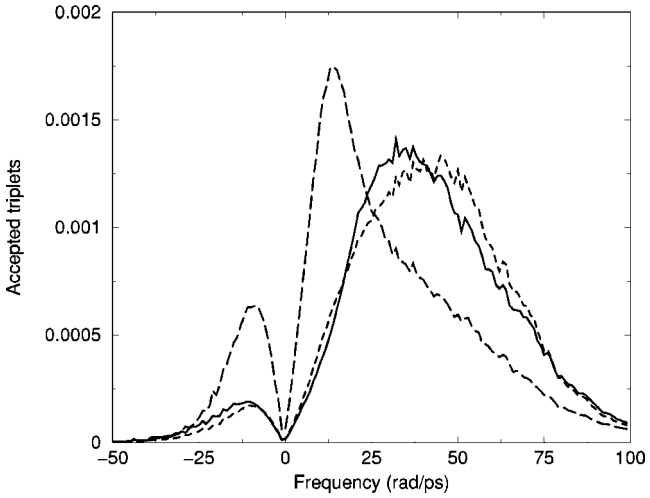

FIG. 6. Projection onto the accepted triplet internal modes. Solid line: asymmetric stretch; short-dashed line: symmetric stretch; dashed line: bending.

dominant at low frequency, where it reaches a maximum at 8 rad/ps, and in the imaginary modes region. The projection along the two stretching modes is anyway interesting. We notice that the projection on the symmetric stretching has a maximum at 23 rad/ps followed by a monotonic decrease. The projection on the asymmetric stretching, that reaches a maximum at a slightly higher frequency of 25 rad/ps, does not show that same behavior; indeed the decrease with increasing frequency after its maximum is followed by a pronounced ''bump'' in the high frequency range. For frequencies higher than 50 rad/ps the projection on the asymmetric stretching mode is almost twice as big as the projection on the symmetric stretching.

The picture emerging from these considerations is that, in methanol, the spectral features in the 25 rad/ps region are due to the stretching of the hydrogen bond, equally shared, at the level of triplet correlations, between the asymmetric and symmetric modes. On the other hand the motions at higher frequency, beyond 50 rad/ps, are dominated by the asymmetric stretching contribution.

B. Water

We present the projection of the INM on the accepted and donated triplets in Figs. 6 and 7, respectively.

The behavior of the three kinds of projections is consistent with the presence of the strong directional hydrogen bonds. The projection on the bending motion, the one less effected by the H-bond restoring force, is indeed predominant at low frequency, where it has a peak at $\omega \simeq 13$ rad/ps for both the accepted and donated triplets.

On the other hand the frequency of the maximum in the projection on the bending mode, 13 rad/ps, coincides with the frequency where a maximum of the longitudinal current spectrum has been found for a wave vector $k > 1$ Å^{-1}, both experimentally[29] and in computer simulation studies.[30] It has already been argued that this feature could be assigned to the O···O···O bending motions.[31] The present analysis is a clear confirmation of this hypothesis.

The bending motion is also the predominant contribution in the imaginary frequency part of the INM spectrum, where it has a peak at $\omega \simeq -10$ rad/ps, where also the projection on the stretching modes exhibits a maximum. Its integrated intensity is 1.5 times higher than the sum of the integrated intensities of the two other modes and this fact shows that the bonded molecules diffuse more likely in the direction perpendicular to the hydrogen bond direction, as might be expected.

The projections on the symmetric and asymmetric stretching modes, on the other hand, are the predominant contribution at high frequencies. In the case of accepted triplets (Fig. 6) we notice that the projection on the asymmetric stretching mode has a peak at $\omega \simeq 35$ rad/ps, whereas the projection on the symmetric stretching mode is maximum at $\omega \simeq 40$ rad/ps. The opposite behavior is observed in the projection of the donated triplets: the symmetric stretching has a peak at $\omega \simeq 35$ rad/ps, which is lower than the frequency of the maximum of the projection on the asymmetric stretching, occurring at $\omega \simeq 45$ rad/ps, probably due to the fact that the

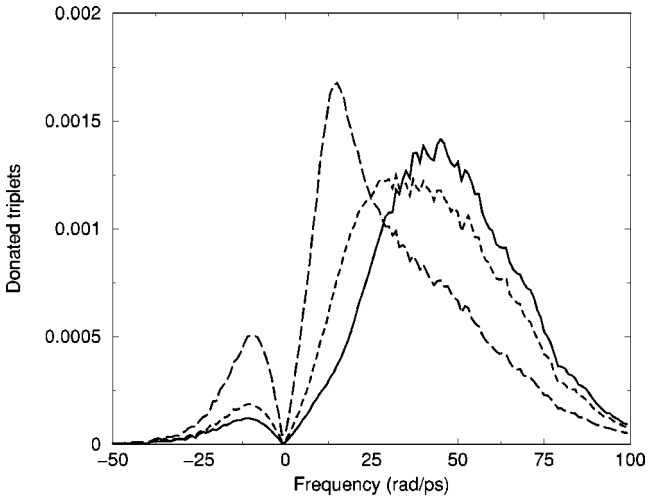

FIG. 7. Projection onto the donated triplet internal modes. Solid line: asymmetric stretch; short-dashed line: symmetric stretch; dashed line: bending.

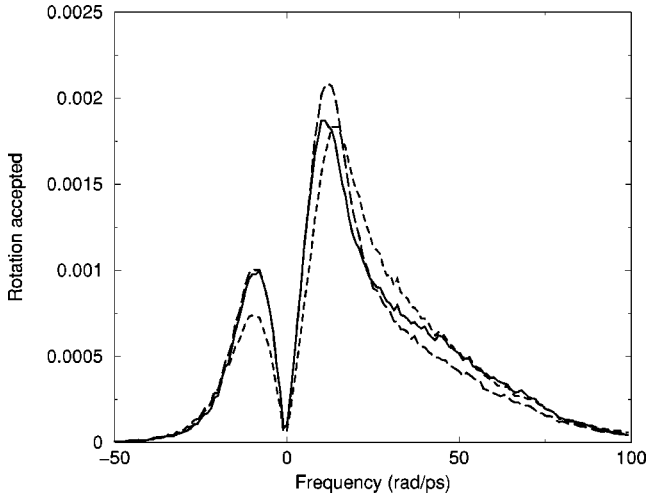

FIG. 8. Projection onto the accepted triplet rigid rotational modes. Solid line: rotation around the ξ_C vector; short-dashed line: rotation around the η_C vector; dashed line: rotation around the axis perpendicular to the triplet plane (ζ_C).

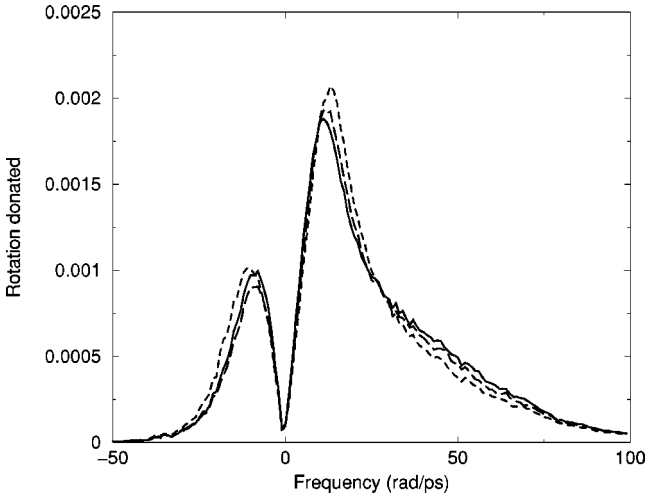

FIG. 9. Projection onto the donated triplet rigid rotational modes. Solid line: rotation around the ξ_C vector; short-dashed line: rotation around the η_C vector; dashed line: rotation around the axis perpendicular to the triplet plane (ζ_C).

two kind of triplets have different geometrical properties (cf. Fig. 3). This result is consistent with previous findings,[25] although a different expression for the projection on the internal modes was used, which, according to the present definition, turns out to be a superposition of internal and rotational modes.

We notice that the frequency of the maxima of the stretching modes are in the same frequency range where Raman peaks have been observed experimentally.[32–34]

A careful inspection of Figs. 6 and 7 shows that the projection on the bending mode has a significant overlap with the projection on the two stretching modes. This is due to the fact that, as already observed, the spatial disposition of the triplets in the liquid does not possess the perfect triangular symmetry that we have used to derive the *a priori* modes [cf. Fig. 3(a)]. Furthermore, the molecules belonging to a triplet are coupled with other molecules in the network and consequently each frequency range contains contributions from every *a priori* mode.

Nevertheless the projection on the *a priori* modes gives a useful indication of the frequency ranges where the bending or stretching character of the actual molecular motion is more pronounced. In particular it can be concluded that the low frequency molecular motions ($\omega < 25$ rad/ps) are dominated by a ''bending'' contribution and the higher frequency ones by the ''stretching'' of the hydrogen bond.

We have also projected the INM motions on the rigid rotation modes of the cluster, and we show the results for accepted and donated triplets in Figs. 8 and 9, respectively. The axes of rotation we have chosen are ξ_C which is directed from the central molecule toward the triplet center-of-mass, ζ_C which is perpendicular to the plane defined by the three molecules, and η_C which is orthogonal to the previous two (cf. Fig. 1).

In this case the difference between accepted and donated triplets is less evident than in the case of the projection on the internal modes. All the projections have an imaginary frequency peak at $|\omega| \simeq 10$ rad/ps and a real frequency peak at $\omega \simeq 12$ rad/ps. This last finding is consistent with the results of Ref. 25, where it was pointed out that the spectrum of the librational motion of the triplets is peaked at 12 rad/ps.

We also notice that in the case of the imaginary modes of the accepted triplets, the projection on the rotation around the η_C axis is slightly lower than the other two, while in the case of donated triplets the three projections are almost indistinguishable. We wish to point out that the contribution of the imaginary modes from the projection on the rotational motions is of the same order of magnitude than the one observed from the projection onto the bending mode. This suggests that diffusion processes are likely to involve a rigid rotation of the triplet.

V. PENTAMER MOTIONS

As is well known the local coordination number of water is very near to 4 and the nearest neighbors of a central molecule are arranged in a tetrahedral structure. It is then natural to extend the analysis based on the triplets to these kinds of clusters. The analysis of the pentamer internal motions confirms the conclusions reached so far and a more detailed view of the origin of the vibrational motions will be obtained.

A. Projection on the INM

The projection of the INM onto the internal modes of a pentamer, according to Eq. (30), is presented in Fig. 10.

As is apparent, even if each contribution extends in the whole range of frequencies, the low frequency region is dominated by the projection onto the bending and torsion modes, whereas the projections onto the symmetric and asymmetric stretching modes contribute mostly in the higher frequency range, being peaked at $\omega \simeq 25$ rad/ps and $\omega \simeq 50$ rad/ps, respectively.

This detailed separation of the INM DOS gives a further indication on the origin of the features observed in the projection on the triplet modes (cf. Figs. 6 and 7). The low

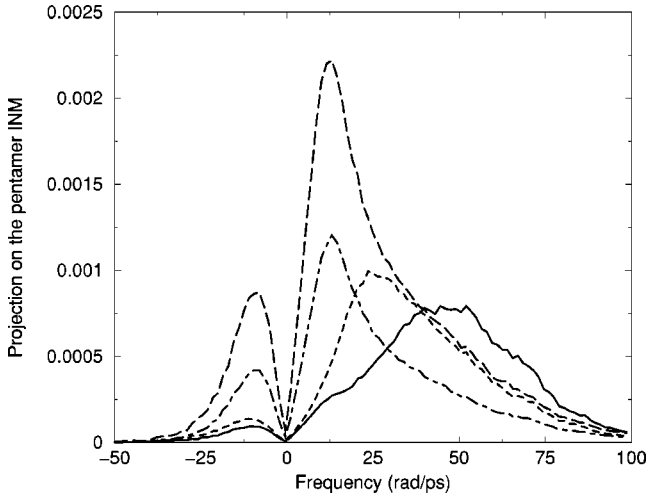

FIG. 10. Projection on the *a priori* modes of water pentamers. Solid line: asymmetric stretching; short-dashed line: symmetric stretching; dashed line: torsion, dotted–dashed line: bending.

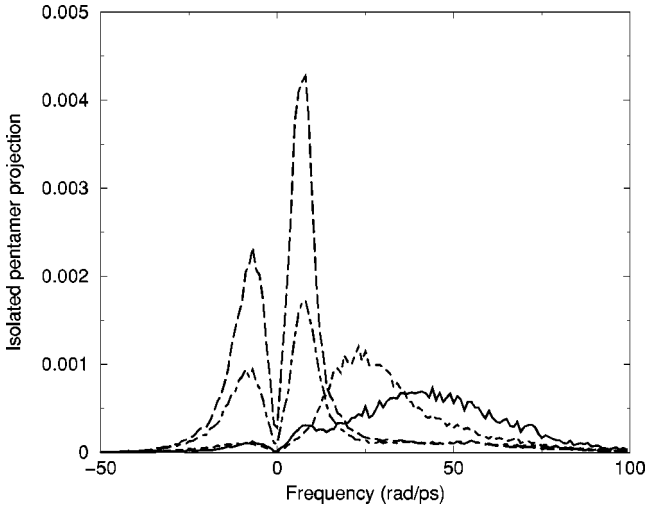

FIG. 11. Projection on the *a priori* modes of isolated water pentamers. Solid line: asymmetric stretching; short-dashed line: symmetric stretching; dashed line: torsion; dotted–dashed line: bending.

frequency bending motion observed in the triplet projection is indeed due to the torsion and bending modes of the underlying pentamer structure, whose contributions have a peak at $\omega \simeq 13$ rad/ps.

On the other hand the two pentamer stretching motions, which appear in the triplet projection as two superimposed bands peaked at $\omega \simeq 35$ rad/ps (cf. Figs. 6 and 7), are resolved in the pentamers into two separate contributions peaked at $\omega \simeq 25$ rad/ps and $\omega \simeq 50$ rad/ps for the symmetric and asymmetric stretching, respectively.

We notice, however, that in the high frequency range there is also a significant projection on the bending and torsion motions, which is comparable to the projection on the asymmetric and symmetric stretching modes. We believe, and demostrate in the following, that this behavior is due to the fact that, in the liquid phase, the vibrational motions of the pentamers at different frequencies always present a mixed character, with respect to the *a priori* modes deduced on the basis of symmetry considerations. This strong mixing is mostly due to the interaction of a pentamer with the molecules in the surrounding environment.

This result could explain why the Raman spectra of water do not show distinct peaks related to the *a priori* motions expected on the local tetrahedral structure.[32] However the present analysis confirms that the two peaks in the Raman spectra at low frequency ($\simeq 12$ rad/ps) and at high frequency ($\simeq 35$ rad/ps) can be assigned to the O···O···O bending mode and to the O···O stretching motion of the triplets, respectively.

B. Projection on the isolated pentamers

We already stressed that the *a priori* modes give only an approximate description of the ''localized normal modes'' present in the liquid, the degree of approximation being due to the interaction of the selected clusters with their neighbors.

In order to demostrate and analyze the effect of this interaction we have calculated and diagonalized the 30×30 Hessian matrices obtained by considering only the interactions between the five pentamer molecules and projected the resulting ''isolated pentamer instantaneous modes'' into the *a priori* modes.

We show the results in Fig. 11, where three frequency ranges can easily be identified. In the low frequency range ($\omega < 15$ rad/ps) the dynamics is dominated by the bending and torsion modes. In the range $15 < \omega < 35$ rad/ps the major contribution comes from the projection on the symmetric stretching mode (which has a peak around 25 rad/ps), while at high frequency the larger contribution comes from the asymmetric stretching mode, with a peak around 45 rad/ps.

A comparison between the results reported in Figs. 10 and 11 clearly shows the effect of the interaction with the surrounding molecules on the internal dynamics of water pentamers, i.e., a strong mixing of the bending and torsion modes with the other two beyond 20 rad/ps, in particular with the symmetric stretching mode which completely overlaps with the torsion mode when the full interaction is taken into account.

VI. CONCLUSIONS

In this paper we have presented the analysis of the correlated motions of clusters of hydrogen bonded molecules in liquid hydrogen fluoride, methanol, and water, by performing suitable projections of the Instantaneous Normal Modes on *a priori* cluster modes derived, for each liquid, on the basis of symmetry considerations of the local hydrogen bond structure.

In the case of HF, the presence of the hydrogen bonded structure is found to be responsible for the high frequency motions, as already discussed in a previous work.[15] The projections on the symmetric and asymmetric stretch modes play an almost equal role.

In the case of methanol we have demonstrated that the hydrogen bond interaction between nearest neighbor molecules induces motions at two different frequencies, though the topology of the hydrogen bond network is linear as in

HF. At frequencies around 25 rad/ps the molecular motion is determined by the stretching of the hydrogen bonds, the symmetric and asymmetric part contributing with the same intensity. The very high frequency motions ($\omega > 50$ rad/ps) are determined almost entirely by the asymmetric stretching motion of three hydrogen bonded molecules.

The presence of two characteristic stretching frequencies in methanol and one in hydrogen fluoride can be ascribed to the different shape of the molecules; the HF molecule is linear and the hydrogen bond is almost in the direction of the molecular axis, whereas the methanol molecule is planar. As a consequence the local motions are possibly influenced by the presence of the methyl group.

In the case of water we have analyzed the relation between the hydrogen bond structure and short-time dynamics from two complementary points of view. Each water molecule is surrounded, on the average, by four molecules, so that the local symmetry of the hydrogen bond network is tetrahedral. Triplets can be easily identified, since each water molecule accepts two bonds from a pair (thus forming an accepted triplet) and donates two bonds to another pair (thus forming a donated triplet).

In both cases we have shown to which extent the different *a priori* motions are dominant at different frequencies. The bending motions are mostly present at low frequencies ($\omega < 25$ rad/ps, with a peak at 13 rad/ps), whereas the stretching motions give the predominant contribution in the frequency range 35–45 rad/ps, very near to the experimentally observed O···O stretching mode.

We have also taken into account the projection of the Instantaneous Normal Modes on the structures representing the full tetrahedral symmetry of the hydrogen bond network, namely the pentamers. In this case we have noticed the presence of a strong mixing between the *a priori* modes. The low frequency motions are mostly projected on those modes which do not involve the stretching of the hydrogen bonds (i.e., torsion and bending). In the high frequency range ($\omega > 20$ rad/ps) there is indeed a maximum of the projection onto the symmetric and asymmetric pentamer stretching modes, but the bending and torsion modes have also a non negligible contribution.

In order to identify the origin of this mixing we have performed the same analysis on the INM obtained by considering isolated clusters.

One can identify the frequency ranges where each of the *a priori* motions are most important, as one might expect. The low frequency motions are mostly related to the bending and torsion modes (which do not involve H-bond stretching), whereas the high frequency ones are related to the symmetric and asymmetric stretching motions, the former being predominant at intermediate frequencies (cf. Fig. 11).

The presence of the strong mixing could explain the reason why the pentamer modes are hardly resolved experimentally, and the observed high frequency vibrational excitations have been assigned to three molecule correlated motions.[32,33]

In the case of triplet motions the mixing between the *a priori* modes, though present, is not strong enough to avoid a precise classification of the predominant contributions at various frequencies.

This ''mixing'' is also observed in the case of hydrogen fluoride and methanol; taking Fig. 4 as a reference, we notice that the projection on the bending motions, though mostly localized in the low frequency region, has indeed a tail extending up to the highest INM frequency and that the projection on the symmetric stretching exhibits a clear bump at low frequency. Anyway the degree of mixing is not so high to effect the conclusions we have presented for these liquids.

In conclusion, the projection of the INM modes onto the *a priori* modes has proved to be a fruitful approach for the investigation of the kind of molecular motions involved at various frequencies, and mostly relies on the ability of the INM approach to relate dynamical and structural properties.

[1] H. Eugene Stanley and J. Teixeira, J. Chem. Phys. **73**, 3404 (1980).
[2] U. Balucani, G. Ruocco, A. Torcini, and R. Vallauri, Phys. Rev. E **47**, 1677 (1993).
[3] W. Jorgensen, J. Phys. Chem. **90**, 1276 (1986).
[4] P. Jedlovszky and R. Vallauri, Mol. Phys. **93**, 15 (1998).
[5] M. Haughney, M. Ferrario, and I. McDonald, J. Phys. Chem. **91**, 4934 (1987).
[6] T. Yamaguchi, K. Hidaka, and A. Soper, Mol. Phys. **96**, 1159 (1999); **97**, 603(E) (1999).
[7] U. Balucani *et al.*, J. Chem. Phys. **111**, 4663 (1999).
[8] U. Balucani, G. Garberoglio, G. Sutmann, and R. Vallauri, Chem. Phys. Lett. **315**, 109 (1999).
[9] E. Guàrdia, G. Sesé, and J. Padró, J. Mol. Liq. **62**, 1 (1994).
[10] J. Martí, J. Padró, and E. Guàrdia, J. Mol. Liq. **64**, 1 (1995).
[11] J. Alonso *et al.*, J. Mol. Struct. **250**, 147 (1991).
[12] D. Bertolini, G. Sutmann, A. Tani, and R. Vallauri, Phys. Rev. Lett. **81**, 2080 (1998).
[13] J. Alonso *et al.*, J. Chem. Phys. **96**, 7696 (1992).
[14] M. Buchner, B. Ladanyi, and R. Stratt, J. Chem. Phys. **97**, 8522 (1992).
[15] G. Garberoglio and R. Vallauri, Phys. Rev. Lett. **84**, 4878 (2000), cond-mat/0001265.
[16] G. Garberoglio and R. Vallauri, J. Chem. Phys. **115**, 395 (2001).
[17] S. Taraskin and S. Elliott, Phys. Rev. B **56**, 8605 (1997).
[18] M. Ribeiro, M. Wilson, and P. Madden, J. Chem. Phys. **109**, 9859 (1998).
[19] S. D. Bembenek and B. B. Laird, J. Chem. Phys. **114**, 2340 (2001).
[20] R. Murry, J. Fourkas, W.-X. Li, and T. Keyes, J. Chem. Phys. **110**, 10410 (1999).
[21] U. Balucani and M. Zoppi, *Dynamics of the Liquid State* (Oxford Science, Oxford, 1994).
[22] R. Vallauri and F. Bermejo, Phys. Rev. E **51**, 2654 (1995).
[23] P. Jedlovszky and R. Vallauri, Mol. Phys. **92**, 331 (1997).
[24] H. Berendsen *et al.*, J. Chem. Phys. **81**, 3684 (1984).
[25] G. Sutmann and R. Vallauri, J. Phys.: Condens. Matter **10**, 9231 (1998).
[26] W. Press, S. Teulkosky, W. Vetterling, and B. Flannery, in *Numerical Recipes in C*, 2nd ed. (Cambridge University Press, Cambridge, 1992).
[27] M. Cho *et al.*, J. Chem. Phys. **100**, 6672 (1994).
[28] F. Sciortino and P. Tartaglia, Phys. Rev. Lett. **78**, 2385 (1997).
[29] F. Sette *et al.*, Phys. Rev. Lett. **75**, 850 (1995).
[30] U. Balucani, J. Brodholt, and R. Vallauri, J. Phys.: Condens. Matter **8**, 9269 (1996).
[31] S. Sastry, F. Sciortino, and H. E. Stanley, J. Chem. Phys. **95**, 7775 (1991).
[32] G. Walrafen, in *Water: A Comprehensive Treatise* (Plenum, New York, 1972), Vol. 1, Chap. 5.
[33] D. Carey and G. Korenowski, J. Chem. Phys. **108**, 2669 (1998).
[34] N. Agmon, J. Phys. Chem. **100**, 1072 (1996).